Journal of Power Sources 195 (2010) 825–828

Contents lists available at ScienceDirect

Journal of Power Sources

journal homepage: www.elsevier.com/locate/jpowsour

Short communication

Invasion percolation with inlet multiple injections and the water management problem in proton exchange membrane fuel cells

Loic Ceballos[a,b], Marc Prat[a,b,*]

[a] Université de Toulouse; INPT, UPS; IMFT, Avenue Camille Soula 31400, Toulouse, France
[b] CNRS, IMFT 31400, Toulouse, France

ARTICLE INFO

Article history:
Received 11 May 2009
Accepted 8 August 2009
Available online 19 August 2009

Keywords:
Polymer electrolyte fuel cells
Micro-porous layer
Gas diffusion layer
Two-phase flow
Pore network model
Invasion percolation

ABSTRACT

Liquid water transport in the diffusion porous layers of polymer electrolyte membrane fuel cells (PEMFC) is analyzed as a process of quasi-static invasion from multiple interfacial injection sources. From pore network simulations based on a new version of the invasion percolation algorithm it is shown that a porous layer acts as a two-phase filter: the number of breakthrough points is significantly lower that the number of injection points owing to the merging of liquid paths within the porous layer. The number of breakthrough points at the gas diffusion layer/gas channel interface obtained with this model is consistent with the available experimental observations.

1. Introduction

Polymer electrolyte membrane fuel cells (PEMFC) are regarded as one of the most promising devices to solve the energy and environmental pollution issues [1]. As discussed in many works, e.g. [1,2] and references therein, water is essential for the operation of PEMFC and the so-called water management problem is one of the key issue for the operation of PEMFC. The water management problem refers to the fact that the membrane should be sufficiently hydrated whereas excessive condensed water should be avoided in other parts of the device, such as the catalyst layer (CL) or the gas diffusion layer (GDL), so as to maintain a good access of reactant gas to reaction sites. A popular approach to this problem is to rely on numerical simulations so as to predict and to analyse the effects of various parameters on pore blockage by the water. Most of these studies are based on the traditional continuum models describing two-phase flow in porous media. However, there are evidences that this type of model can be seriously in error, notably owing to the thin nature of the porous layers (lack of length scale separation) or because the water flow regime is dominated by capillary effects, a regime which cannot be described using continuum models, see [3] and references therein for more details. As considered in several previous works [3–6], an alternative for a better understanding of water invasion in PEMFC porous layers is to rely on pore network models and associated theories. Since water invasion is dominated by capillary effects and the porous layers are generally assumed as hydrophobic (this aspect is commented at the end of the paper) water invasion in the GDL has been simulated using the invasion percolation (IP) algorithm [7] since it is well established that the capillarity dominated displacement of a wetting fluid (the gas phase in the PEMFC problem) by a non-wetting one (water in the PEFMC problem) can be adequately simulated with the IP algorithm. However, as pointed out in [2] and [3], there is a fundamental difference between the PEMFC problem and the traditional situations involving a drainage (drainage refers to the process of displacing a wetting fluid by a non-wetting one) process at very low capillary numbers in porous media (the capillary number characterizes the competition between capillary and viscous forces, the later can be neglected for a sufficiently small capillary number). In the traditional use of the IP algorithm, all pores at the porous medium inlet are supposed to be connected to a reservoir and the invasion is simulated increasing steps by steps very gently the pressure of the non-wetting fluid in the reservoir. In the PEMFC problem, water entering a porous layer, for example the GDL, comes from an adjacent porous layer, the micro-porous layer (MPL) or the CL, and not from a reservoir at uniform pressure. Hence the injection conditions in the PEMFC problem are markedly different from the traditional injection condition. It is therefore surmised that this has a great impact on the phase distribution and therefore the pore blockage by the water [2,3]. A well-known fact in favour of this fundamental difference is that emergence of several liquid water

* Corresponding author at: Université de Toulouse; INPT, UPS; IMFT Avenue Camille Soula 31400, Toulouse, France. Tel.: +33 561285883; fax: +33 561285899.
E-mail address: prat@imft.fr (M. Prat).

0378-7753/$ – see front matter © 2009 Elsevier B.V. All rights reserved.
doi:10.1016/j.jpowsour.2009.08.029

droplets is generally observed at the GDL/gas channel interface [8–10]. This cannot be predicted when the IP algorithm is used with the traditional "connected reservoir" boundary condition since only one breakthrough droplet is predicted in this case. If condensation effects and viscous effects can be neglected, one obvious possibility for predicting multiple breakthrough points with the IP algorithm is to consider that water enters into a porous layer through multiple independent inlet injection points [2,11]. One argument in favour of this scenario is that the MPL pores are approximately about 100 times smaller than those in the GDL and that the size of pores between the agglomerates in the CL is in turn at least 10 times smaller than the average pore size in the MPL. Because of this hierarchy in pore sizes liquid water produced in the CL can enter the MPL from many pores. This leads to the possibility of formation of several liquid paths into the MPL. If there is no complete merging of those liquid paths inside the MPL, this leads in turn to the possibility of several injection points into the GDL and eventually, if again there is no complete merging of liquid paths within the GDL, to the possible emergence of several droplets at the GDL/gas channel interface. In this article, we explore the relevance of this scenario from IP simulations with a new inlet boundary condition considering that liquid water can enter each porous layer from multiple injection points.

2. IP algorithm with multiple inlet injections

As in a previous work [3], we consider that the size of a unit cell of the system is fixed by the mean distance L between two channels in the bipolar plate (assuming for simplicity a system of parallel channels) with $L \approx 2$ mm. This leads to study the liquid invasion in porous systems of size $L \times L \times \ell$ where ℓ is the porous layer thickness. As discussed in [3], a representative mean distance a between two pores in the GDL can be estimated as $a \approx 50$ μm whereas ℓ is typically in the range [170–400] μm. If for simplicity we do not take into account the GDL microstructure anisotropy (this aspect will be considered in a future work), this leads to the consideration of $40 \times 40 \times N$ pore networks with N varying in the range [4, 40] (with a lattice spacing a of 50 μm, $N = 4$ corresponds for example to a GDL thickness of 200 μm). The MPL is made of particles and has pore sizes of the order of 0.5 μm whereas its thickness is typically in the range 10–20 μm. As a reasonable guess of mean distance between two pores in MPL, we take 2 μm. This leads to $1000 \times 1000 \times M$ pore networks with M varying in the range [5,10] (with a lattice spacing a of 2 μm, $M = 5$ corresponds for example to a MPL thickness of 10 μm). As in [3], the simulations are performed over simple cubic networks of pores connected by throats, with the throat and pore sizes randomly distributed over the network as explained in [3].

Since water is produced in the agglomerates of the CL, i.e. potentially everywhere in the CL, and since the size of secondary pores in the CL (the secondary pores are the pores between the agglomerates) is about 10 times smaller than the pore size in the MPL, we assume here for simplicity that water enters the MPL in liquid form at the CL/MPL interface through all pores of MPL located at the CL/MPL interface. Hence we assume that the number n_{mi} of pores at the CL/MPL interface where liquid water penetrates into the MPL is $n_{mi} = 1000 \times 1000$. In fact we expect that n_{mi} varies with the current density but this would be explored in a future work. To determine the number of breakthrough points n_{mb} at the MPL outlet (MPL/GDL interface), we use the following IP algorithm. We determine the flow path using the standard IP algorithm without trapping [7] starting with only one injection point (the first pore in the first pores row at the MPL inlet). Then we repeat the simulation starting from the second pore in the first row. We stops this second simulation either when the flow path generated from this second injection point merges into the flow path associated with the first inlet injection pore or at breakthrough, i.e. when the liquid injected from the second inlet pore reaches the MPL/GDL interface through a path independent from the path connected to the first injection point. Then we repeat this procedure starting successively from all the other pores at the CL/MPL interface. Spatial periodicity boundary conditions are imposed on the lateral sides of network.

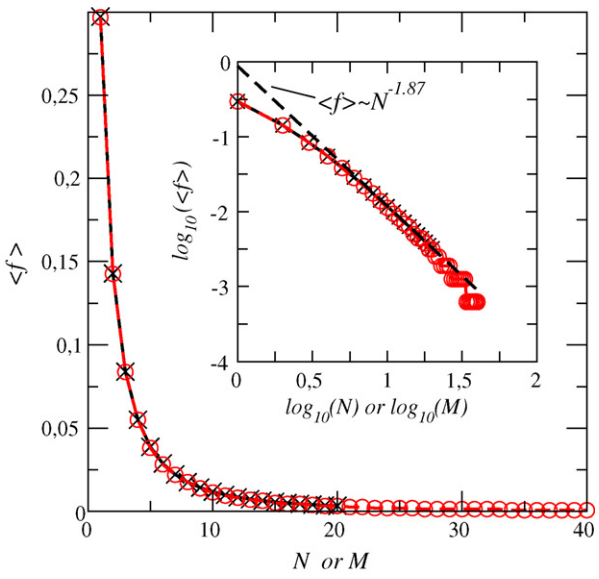

Fig. 1. Evolution of average penetration $\langle f \rangle$ as a function of layer thickness M (MPL) or N (GDL) measured in lattice spacing unit. The results for the MPL $1000 \times 1000 \times M$ networks (black crosses) and for the GDL $40 \times 40 \times N$ networks (red circles) collapse in a single curve except for the larger values of N for which there are less than 10 breakthrough points. The inset shows a log–log plot of the same data together with a best linear fit showing that $\langle f \rangle \sim N^{-1.87}$ for N or $M \geq 6$.

3. Results

So as to take into account the statistical fluctuations inherent to a IP process on a finite size structure, the simulations are performed over 200 realizations, unless otherwise mentioned, of the cubic lattice for each size M considered. The results are analyzed in terms of the "penetration" f (by analogy with particles filtration problems), which is defined as $f = n_{mb}/n_{mi}$. Thus f represents the fraction of pores at the porous medium outlet where a breakthrough occurs, or alternatively the probability that a pore at the porous medium outlet is a breakthrough pore. The evolution of $\langle f \rangle$, where $\langle f \rangle$ is the penetration averaged over the number of realizations considered, is shown in Fig. 1 as a function of M. As can be seen from Fig. 1, $\langle f \rangle$ drops rapidly with M. The MPL acts in fact as a quite efficient two-phase filter since the fraction $\langle f \rangle$ of breakthrough pores at the MPL outlet is significantly lower than 1, even for M as small as 1 for which $\langle f \rangle \approx 0.3$. As shown in the inset in Fig. 1, the variation of $\langle f \rangle$ with M is consistent with a power law of the form $\langle f \rangle = p(\ell/a)^{-1.87}$ with $p \approx 0.882$, except for $M = \ell/a < 6$. It is expected that this scaling holds only over a limited range of M for $M > 6$ since the number of breakthrough pore n_{mb} cannot be lower that 1. This is illustrated further below when the GDL smaller network is considered. This indicates that the merging of liquid flow paths eventually leads to leave many pores free of water and therefore accessible to gas even for the extreme case considered here where all pores at the inlet are injection points. Owing to the randomness in the throats size, the number of breakthrough pores n_{mb}, and therefore the penetration f, are random variables. As will be illustrated below, the probability density function (p.d.f.) of the number of breakthrough points is Gaussian. The values of $\langle n_{mb} \rangle$ and of the standard deviation σ_n of n_{mb} obtained from our simulation are summarized in Table 1.

Table 1
Evolution of average number of breakthrough points $\langle n_{mb} \rangle$ at MPL outlet and standard deviation of n_{mb} as a function of MPL thickness (measured in lattice spacing).

M	$\langle n_{mb} \rangle$	σ_n
1	297320.0	443.0
2	142789.0	290.5
3	83945.8	200.2
4	55020.0	166.5
5	38744.2	127.8
6	28705.4	108.8
7	22096.5	110.7
8	17504.8	87.4
9	14200.7	87.2
10	11741.1	72.91
11	9877.0	63.25
12	8404.0	56.97
13	7249.18	57.71
14	6307.5	50.02
15	5542.54	49.16
16	4907.28	52.64
17	4380.52	41.33
18	3927.34	42.31
19	3538.76	38.94
20	3211.23	35.24

Table 2
Evolution of average number of breakthrough points $\langle n_{gb} \rangle$ at GDL outlet, standard deviation of n_{gb} and breakthrough number density as a function of GDL thickness (measured in lattice spacing).

N	$\langle n_{gb} \rangle$	σ_n	Breakthrough number densities (pores per mm^2)
1	475.4	17.43	119
2	228.4	9.91	57
3	134.8	8.158	33
4	88.07	6.447	22
5	61.67	5.604	15
6	45.87	4.645	11
7	35.76	4.026	8
8	28.12	3.417	7
9	22.93	3.333	5
10	18.67	2.98	4
11	15.82	2.794	3
12	13.63	2.521	3
13	11.61	2.441	3
14	10.23	2.086	2
15	8.72	2.018	2
16	7.88	1.961	1.75
17	7.1	1.944	1.75
18	6.415	1.686	1.5
19	5.805	1.666	1.25
20	5.285	1.563	1.25
21	4.725	1.562	1
22	4.075	1.375	1.
23	3.84	1.365	0.75
24	3.665	1.274	0.75
25	3.265	1.29	0.75
26	3.08	1.214	0.75
27	2.87	1.124	0.50
28	2.76	1.115	0.50
29	2.665	1.001	0.50
30	2.42	1.115	0.50
31	2.32	0.9042	0.50
32	2.175	0.8913	0.50
33	2	0.8544	0.50
34	1.855	0.7576	0.25
35	1.78	0.7427	0.25
36	1.795	0.7956	0.25
37	1.645	0.7609	0.25
38	1.645	0.7064	0.25
39	1.55	0.6225	0.25
40	1.395	0.5648	0.25

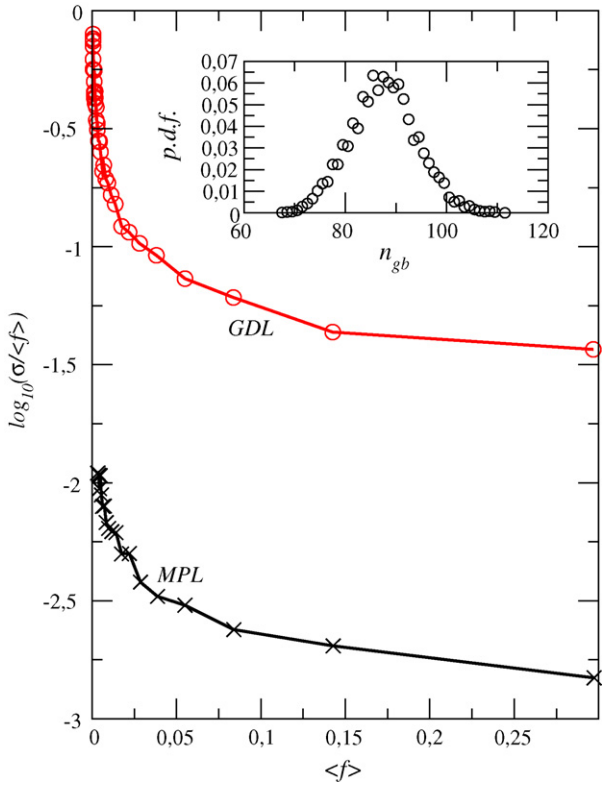

Fig. 2. Semi-log plot of standard deviation σ of penetration f as a function of average penetration $\langle f \rangle$ (the red solid line with crosses corresponds to the GDL $40 \times 40 \times N$ networks whereas the black solid line with circles is for the MPL $1000 \times 1000 \times M$ networks). The inset shows the p.d.f. (probability density function) of n_{gb} for $N = 4$ obtained from 5000 realizations of the GDL network.

To determine the number of breakthrough points n_{gb} at the GDL outlet, we use the same IP algorithm as before. A possible essential difference is that not all pores at the GDL inlet (MPL/GDL interface) are necessarily injection points since water exits the MPL through a limited number of breakthrough points, see Table 1. As noted before, the mean distance between two pores is of the order of 2 μm in the MPL and 50 μm in the GDL. The simulations show that the breakthrough points are randomly distributed over the MPL outlet surface. Hence when the number of breakthrough points n_{mb} at the MPL outlet is lower than $40 \times 40 = 1600$, a reasonable assumption is that there is n_{mb} injection pores into the GDL since it is likely that each breakthrough points from the MPL is connected to a different pore of the GDL at the MPL/GDL interface, that is $n_{gi} = n_{mb}$. When n_{mb} is greater than 1600, then several MPL breakthrough pores can be connected to the same interfacial pore of the GDL and therefore $n_{gi} = 1600$ since n_{gi} cannot be greater than 1600. The values reported in Table 1 show that n_{mb} is greater than 1600 for the range of MPL thickness considered and when all MPL inlet pores are injection pores. We therefore explore first the case $n_{gi} = 1600$.

The evolution of average penetration $\langle f \rangle$ for the GDL network is shown in Fig. 1 (red line with circles) while the inset in Fig. 1 shows the same data in log–log coordinates. As can be seen there is a perfect collapse of the data obtained from the MPL $1000 \times 1000 \times M$ network and from the GDL $40 \times 40 \times N$ network except for the larger values of N for which the number of breakthrough points becomes lower than 10, that is too small for observing a quasi-continuous evolution of $\langle f \rangle$ with N. Hence the staircase evolution of $\langle f \rangle$ reflects the fact that there are only a few breakthrough points for the larger N (see Table 2). As mentioned before and shown in the inset in Fig. 2, the p.d.f of the number of breakthrough pores is Gaussian. Contrary to the evolution of $\langle f \rangle$, which is independent of

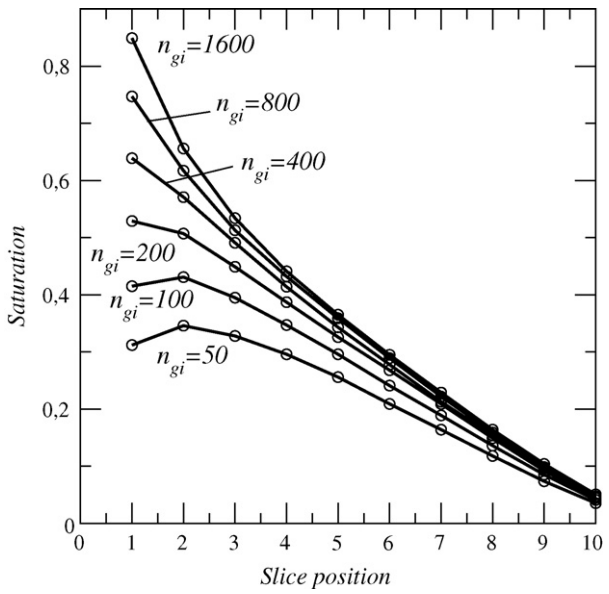

Fig. 3. Water saturation profiles along the GDL for $N = 10$ for various average number of inlet injection points n_{gi} (1600, 800, 400, 200, 100, 50) randomly distributed over the GDL inlet face. Each profile is an average over 200 realizations of the GDL network. The saturation fluctuations are small, so that a variation of one standard deviation about the average values would not be discernible in the figure.

L/a, there is a significant effect of network size L/a on the standard deviation of f. This is shown in Fig. 2. As can be seen, $\sigma_f/\langle f\rangle$ decreases with network size with $\sigma_f/\langle f\rangle$ in the range $[10^{-3}, 10^{-2}]$ for $L/a = 1000$ and $\sigma_f/\langle f\rangle$ two orders of magnitude greater for $L/a = 40$. This aspect will be explored in more detail in a forthcoming work.

The breakthrough density d_n (number of breakthroughs per unit area) at the GDL outlet (GDL/channel interface) obtained in our simulations is reported in Table 2. As can be seen, $\langle d_n\rangle$ is in the range [4–22] pores per mm^2 for porous layer thicknesses representative of those of GDLs. This is in very good agreement with the observations of droplet formations at the GDL/channel interface reported in [10].

As a final result, Fig. 3 shows the liquid saturation profiles along the GDL thickness for $N = 10$. These profiles are obtained by determining the saturation in successive slices of the network along the GDL thickness. As stated before, it can be surmised that the number of injection points varies with the current density. So as to have a first insight into the impact of the number of injection points, the profiles corresponding to various average numbers of injection points are shown in Fig. 3. Interestingly, the profile shape changes from concave to convex as the number of injection points decreases. As discussed for example in [3,11], the shape of the saturation profile is an important indication as regards the analysis of two-phase flow in GDL. Hence our results can explain why profiles deduced from in situ experiments [12,13] are not concave. Also, it can be seen from Fig. 3 that the saturations along the GDL thickness are here significantly greater than when the traditional "connected reservoir" boundary condition is used (see for example Fig. 14 in [3]), especially in the second half of profiles.Hence the traditional use of the IP model with the "connected reservoir" boundary condition leads to seriously underestimate the pore blockage by the water. The inlet independent injection points boundary condition appears as much more appropriate for analyzing two-phase flows in a GDL as well as in the MPL.

4. Conclusion

We have explored a possible scenario of droplet generations at the GDL/gas channel interface assuming that water invasion into the GDL and the MPL could be described using the IP algorithm. Contrary to classical IP simulations, the present simulations are based on the concept that liquid water enters the porous layer through multiple independent injection sources at the inlet. The results are consistent with the available data on the density of droplets forming at the GDL/gas channel interface as well as with the saturation profile shape observed in in situ experiments. The algorithm proposes in this article provides one tool to better analyze the water management problem in PEMFC. However, the droplets generation process at the surface of a porous layer described in this article is probably not the only one taking place in PEMFC. Condensation processes (more likely however on the anode side than on the cathode side [2]) and viscous effects [11] (neglected in the present effort) could also play a role in the droplet formations. Also, we have assumed perfectly hydrophobic porous layers and isotropic microstructures. As considered for example in [14], there are evidences that the GDL is only partially hydrophobic and it is well known that the GDL microstructure is not isotropic. The effects of a mixed wettability and anisotropy on droplets generations would deserve to be explored using an approach similar to the one described in this article.

Acknowledgements

Financial supports from GIP ANR (project ANR-06-PANH-022-02 "Chameau") are gratefully acknowledged.

References

[1] F. Barbir, PEM Fuel Cells: Theory and Practice, Elsevier Academic Press, 2005.
[2] J.H. Nam, K.J. Lee, G.S. Hwang, C.J. Kim, M. Kaviany, Int. J. Heat Mass Transfer 52 (2009) 2779.
[3] M. Rebai, M. Prat, J. Power Sources 192 (2008) 534, available online 14 March.
[4] O. Chapuis, M. Prat, M. Quintard, E. Chane-Kane, O. Guillot, N. Mayer, J. Power Sources 178 (2008) 258.
[5] J.T. Gostick, M.A. Ioannidis, M.W. Fowler, M.D. Pritzker, J. Power Sources 173 (2007) 277.
[6] V.P. Schulz, J. Becker, A. Wiegmann, P.P. Mukherjee, C.Y. Wang, J. Electrochem. Soc. 144 (4) (2007) B419.
[7] D. Wilkinson, J.F. Willemsen, J. Phys. A-Math. Gen. 16 (1983) 3365.
[8] K. Tüber, D. Pocza, C. Hebling, J. Power Sources 124 (2003) 403.
[9] X.G. Yang, F.Y. Zhang, A.L. Lubawy, C.Y. Wang, Electrochem. Solid-State Lett. 7 (11) (2004) A408.
[10] F.Y. Zhang, X.G. Yang, C.Y. Wang, J. Electrochem. Soc. 153 (2) (2006) A225.
[11] K.J. Lee, J.H. Nam, C.J. Kim, Electrochim. Acta 54 (2009) 1166.
[12] M.A. Hickner, N.P. Siegel, K.S. Chen, D.S. Hussey, D.L. Jacobson, M. Arif, J. Electrochem. Soc. 155 (2008) B427.
[13] C. Hartnig, I. Manke, R. Kuhn, N. Kardjilov, J. Banhart, W. Lehnert, Appl. Phys. Lett. 92 (2008) 134106.
[14] H. Chraibi, L. Ceballos, M. Prat, M. Quintard, A. Vabre, Proceedings of Fundamentals & Developments of Fuel Cells (FDFC) 2008 Conference, Nancy, December 10–12th, 2008.